Nature Environment and Pollution Technology
An International Quarterly Scientific Journal

p-ISSN: 0972-6268 (Print copies up to 2016)
e-ISSN: 2395-3454

Vol. 20 | No.3 | pp. 1087-1096 | 2021

Original Research Paper
https://doi.org/10.46488/NEPT.2021.v20i03.016
Open Access Journal

# Spatial and Temporal Characteristics of $PM_{2.5}$ Sources and Pollution Events in a Low Industrialized City

**R. Xu*, Q. Tian*, H. Wan**†, J. Wen***, Q. Zhang* and Y. Zhang***
*College of Computer and Information Security, Guilin University of Electronic Technology, Guilin 541004, China
**Key Laboratory for City Cluster Environmental Safety and Green Development of the Ministry of Education, Institute of Environmental and Ecological Engineering, Guangdong University of Technology, Guangzhou, 510006, China
***Guilin Environmental Monitoring Center Station, Guilin 541002, China
†Corresponding author: H. Wan; wanhang@gdut.edu.cn

Nat. Env. & Poll. Tech.
Website: www.neptjournal.com

*Received:* 28-08-2020
*Revised:* 04-11-2020
*Accepted:* 08-12-2020

**Key Words:**
$PM_{2.5}$
Air pollution
Pollution events
Spatial characteristics

## ABSTRACT

In recent years, cities in southern China have experienced severe air pollution, despite having few sources of pollutants. To study the pollution characteristics of $PM_{2.5}$ in these "low industrialized" cities, a numerical method based on the HYSPLIT4 Model and Kriging Spatial Interpolation Technology was established. Simulation results showed that the $PM_{2.5}$ pollution in Guilin was affected by both internal and external sources. The backward air mass trajectory from July 2017 to June 2018 was simulated using the HYSPLIT model. The cluster analysis results indicated that the direction of trajectory ② accounted for 63.09% of the air pollution in the city. The average concentration of $PM_{2.5}$ pollution was 45.94 $\mu g.m^{-3}$. The pollutant originated from the "Xiang-Gui Corridor." The location of the sources was collocated with high industry regions. The spatial characteristics of the four pollution processes in the winter of 2017 were analyzed using a spatial interpolation method. The results showed that the transport of air masses in the direction of trajectory ② was obstructed by a mountain system in the northeast. Therefore, two air pollution accumulation centers and a topographic weakening zone dominated by internal and external sources were formed. It can be inferred that the air pollution in Guilin is affected by both internal and external factors. These results provide important theoretical and technical support for regional air pollution control and environmental protection.

## INTRODUCTION

The Chinese government implemented a series of air pollution prevention and control measures to improve the country's air quality. Under this situation, air quality in most regions has improved, but pollution remains serious in some areas (Luan et al. 2018, Jiang et al. 2018, Cui et al. 2019, Sun et al. 2019). It is worth noting that tourist areas in southern China, such as Guilin, have also suffered serious air pollution, despite having fewer sources of pollutants. However, there is no clear conclusion about the cause of air pollution in tourist areas, which are quite different from those in industrial cities because of their characteristics. In recent years, with the development of tourism, the eco-environmental problems in Guilin have been a cause of concern for environmental workers. Bai et al. (2017) studied the impact of climate re( sources on the tourism development of Guilin International Resort and found that air pollution would affect tourism development. As a tourism city, ensuring the air quality of Guilin is necessary and important.

Scholars adopted several tools to analyze the sources of air pollutants and characterize pollution characteristics. For example, Zhang et al. (2019) employed the Comprehensive Air Quality Model Extensions (CAMx) based on the Particulate Source Apportionment Technology (PSAT) to simulate and analyze the sources of $PM_{2.5}$ in Beijing. They found that 47.6% of the $PM_{2.5}$ originated from local sources. Zhang et al. (2018) used the Community Multiscale Air Quality Modeling System (CMAQ) to simulate the changes of surface $PM_{2.5}$ in Qingdao during winter. They found that $PM_{2.5}$ accounted for 72.7%–93.2% of the daily emissions. This percentage would decrease by about 21% when considering the pollution process, and the proportion of aerosol accumulation would increase by about 6%. Another study by Yang et al. (2019) used the WRF-SMOKE-CMAQ model to analyze the life cycle of $PM_{2.5}$ in Xi'an from 2014 to 2017. The study concluded that the $PM_{2.5}$ concentrations increased from 82.4 $\mu g.m^{-3}$ to 95.4 $\mu g.m^{-3}$ as a result of dust emissions into the atmosphere. Wang et al. (2015) analyzed the air pollution in the Yangtze River Delta in December 2013 using a Principal Component Analysis (PCA). They found that the concentration of fine particulate matter increased due to the anthropogenic emission of dust from Northwest China. This method of research uses a meteorological grid, which needs to be analyzed with an internal source list data. This research model is suitable for the pollution source analysis of large-scale regions but is ineffective when extrapolating the source of a pollutant from pollution monitoring points.

The Hybrid Single-Particle Lagrangian Integrated Trajectory (HYSPLIT) model can be used to trace the transport and diffusion trajectory of pollutants from the monitoring points. Arif et al. (2018) used the HYSPLIT4 model to study the source of atmospheric pollutants in Patna in 2015. The Concentration Weighted Trajectory (CWT) method was also used to analyze pollution levels in source regions. Mukherjee and Agrawal (2018) studied the sources of $PM_{2.5}$ pollution in Varanasi, India, from 2014 to 2017. They quantified the contribution from traffic, road dust, and internal combustion activities, and found that Northwest India was the main source area. Liu et al. (2013) used the CWT method to track the origin and transport of atmospheric pollutants in Lanzhou. Results showed that the HYSPLIT model and CWT analysis methods are effective tools when analyzing external sources and their corresponding contributions (Sun et al. 2015, Perrone et al. 2018). However, it is difficult to clarify the temporal and spatial characteristics of air pollution processes under the combined action of internal and external sources in small-scale regions.

The internal sources of air pollution are studied using set pair analysis and the spatial interpolation method used by some scholars. Zhou et al. (2016) constructed the set pair analysis method for internal and external sources of $PM_{2.5}$ and then studied the proportion of internal to external sources in Dongguan. However, this study did not consider the spatial and temporal characteristics of the pollutants. Yang et al. (2018) employed a Spatiotemporal Ordinary Kriging (STOK) technique and analyzed the daily concentrations of $PM_{2.5}$ in southern Jiangsu province in 2014. Their results showed that 29.3% of the area was polluted by $PM_{2.5}$ in 2014. Additionally, the number of polluted days varied from 59 to 164 in different parts of the study region. The spatial interpolation method can be used to study the spatial and temporal distribution of pollutants, but previous studies typically focused on the correlation between a pollutant and various meteorological parameters. The correlation analyses speculated the causes of regional pollution but failed to consider that transport, emissions, and accumulation are affected by topography.

Previous studies failed to capture the complete life cycle of a pollutant (Zdun et al. 2016, Zhao et al. 2015, Liu et al. 2017). To fully understand the emission and transport of pollution, this study needs to track the trajectory of a pollutant, locate and quantify its sources, and consider the effects of topography. In this paper, the HYSPLIT method is adopted to determine the trajectory of an air mass and estimate air pollution sources. Then, the PSCF and CWT methods are used to quantify and analyze the internal pollution sources. Furthermore, spatial interpolation and topographic element methods are adopted to determine the temporal and spatial distribution characteristics of pollutants.

## MATERIALS AND METHODS

### Study Object and Data

Guilin was selected as the research area. Guilin covers an area of 27,809 $km^2$ and has a population of over 5 million. The research area borders Yongzhou and Shaoyang of Hunan Province in the northeast and Liuzhou in the south. All three are heavy industrial cities.

The topographical distribution of the study area is presented in Fig. 1. The west, north, and southeast regions are mountainous and have higher terrain. The central regions have relatively low terrain. There is a long narrow channel in the northeast between the Yuechengling and Dupangling-Haiyangshan Mountain chains. The depth of this channel, also known as the "Xiang-Gui Corridor," ranges from 600 to 1600 m between the mountain peak and the basin.

Guilin has lower pollution emissions than surrounding cities, but its air quality is significantly worse. The overall amount of $PM_{2.5}$ remains high, especially in Quanzhou County, Pingle County, Yongfu County, and downtown Guilin.

The research area contains 19 fixed atmospheric environmental quality automatic monitoring stations ("fixed stations" in short) and 51 mini ones ("mini stations" in short). Guilin University of Electronic Technology Yaoshan Station (Yaoshan Station) was selected as the background value reference station because it was considered to be free from the influence of internal sources. Yaoshan Station is 13 km from downtown Guilin. Vegetation covers more than 78% of this station, and consequently, this station is only weakly influenced by the air pollution from downtown.

The following basic data was used to analyze the sources and spatial distribution of air pollution in the research area: hourly average data of the 19 fixed stations in Guilin, including wind direction, wind speed, temperature, rainfall, barometric pressure, humidity, and $PM_{2.5}$ concentration; Landsat8 satellite 30 m resolution full-band image, administrative division data, and elevation DEM image data provided by Geographic Cloud; and the GDAS data (spatial resolution 1°×1°) provided by US National Centers for Environmental Prediction (Table 1).

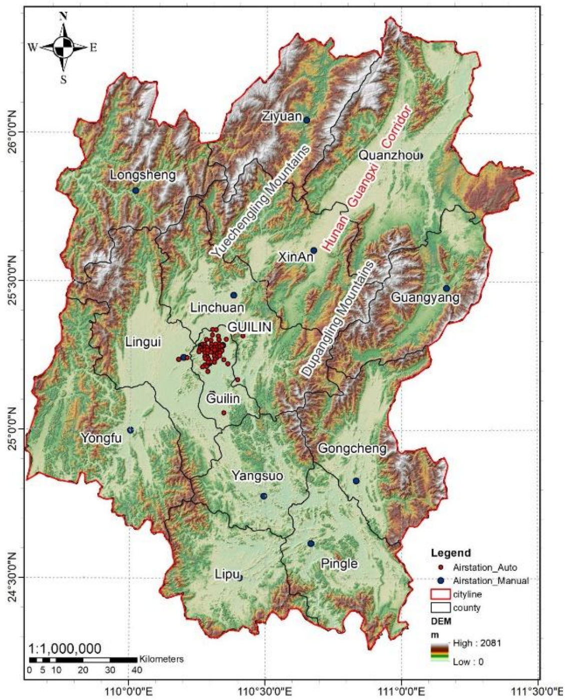


Fig. 1: Topography of the study area and distribution of monitoring stations.

Table 1: Datasheet.

| Data category | Data contents | Data source | Time range | Resolution |
|---|---|---|---|---|
| Meteorological data | $PM_{2.5}$ | Guilin Environmental Monitoring Station | 2014.3–2019.6 | Day |
| Meteorological analysis data | Wind speed, wind direction, temperature, rainfall, barometric pressure, moisture content | Guilin Environmental Monitoring Station | 2017.7–2018.6 | Day |
| Air mass trajectory data | GDAS data | NCEP | 2017.7–2018.6 | 1°×1° |
| Geographic data | DEM data, Administrative division data | China Geographic cloud space website | 2017.7–2018.6 | 30m×30m |

## Study Methods

The internal and external sources and the transport pattern of the air pollutants in the research area were analyzed using the data described above. First, the trajectory of the air mass was simulated for 365 consecutive days using the HYSPLIT4 model. Using a spatial clustering method, it was found that air pollution was transported from several directions. Second, the PSCF method was used to grid the potential source areas. Third, the CWT method was employed to quantify the grid value of the pollutants in the potential source areas. Fourth, four periods with severe pollution were selected. The changes of $PM_{2.5}$ were calculated using the spatial interpolation method, which analyzed the spatial and temporal distributions of pollutants. Finally, the temporal and spatial characteristics of air pollution in the study area under the influence of meteorological and topographic changes were discussed.

## External Source Transmission

The HYSPLIT4 model was used to simulate the trajectory of an air mass for continuous periods to determine the direction of air pollutant transmission from external sources. The HYSPLIT4 model is a hybrid single-particle orbit model developed by the Air Resources Laboratory (ARL) under the US National Oceanic and Atmospheric Administration (NOAA). This model is used to calculate and analyze the trajectories of atmospheric pollutants and diffusion. Trajectories were categorized according to their spatial variation

(SPVAR) to obtain the relationship between the total spatial variation (TSV) (the sum of SPVAR) and n (the number of trajectories). Based on the clustering results, the locations of source regions were determined using the PSCF method. Then CWT method was used to quantify the pollution weight and thus estimate the total pollutants carried out.

(1) Potential Source Contribution Function - PSCF

The PSCF method determines the location of a pollution source by setting the atmospheric backward trajectory and the meteorological values. The PSCF function is defined as the conditional probability that the value of an element corresponding to the monitoring grid, namely $PM_{2.5}$ concentration, exceeds the set threshold when an air mass passing through an area reaches the monitoring grid. The PSCF value of the *i-th* grid within the research area is shown in Equation (1):

$$PSCF_i = \frac{m_i}{n_i} \quad \ldots(1)$$

where $n_i$ and $m_i$ separately represent the relative standing time of backward air quality and pollutant concentration in the retention area. The PSCF method calculates the contribution of the grid to pollutant concentrations in the research area.

(2) Concentration-Weighted Trajectory (CWT)

The PSCF method can determine the correlation between the corresponding element value and the threshold value of the trajectory in the grid. Therefore, the CWT method is used to quantify and analyze the weighted concentration of pollutants. The weighted concentration of grid *i* refers to the time-averaged concentration of monitoring points passing through grid *i*, as shown in Equation (2):

$$CWT_i = \frac{1}{\sum_{l=1}^{t} n_{il}} \sum_{i=1}^{t} C_{il}, \quad \ldots(2)$$

Where $CWT_i$ denotes the weighted concentration of grid *i*, *l* denotes the serial number of the trajectories, *t* denotes the total number of trajectories, $n_{il}$ denotes the time spent by *l-th* trajectory passing through grid *i*, and $C_{il}$ is the $PM_{2.5}$ concentration of trajectory *l* while passing through grid *i*.

## Internal Source Diffusion

A spatial interpolation method was used for the internal source diffusion analysis. The regional changes in concentration were estimated, and the influence of internal sources was analyzed, as were the topographic characteristics.

If it is assumed that there are *n* points of actual measurements within the area of point $x_0$, namely $x_1, \ldots, x_n$. Then, the Kriging interpolation method is expressed as Equation (3):

$$Z^*(x_0) = \sum_{i=1}^{n} P_i Z(x_i), , \quad \ldots(3)$$

where $Z^*(x_0)$ denotes the concentration grid values of $PM_{2.5}$; *n* stands for the number of stations used for $PM_{2.5}$ interpolation; $Z(x_i)$ is the average $PM_{2.5}$ concentration of *i-th* station, and $P_i$ is the undetermined weighting coefficient. After the unbiased minimum variance estimation is executed, Equation (4) is derived by introducing the Lagrange coefficient *Q*:

$$\sum_{i=1}^{n} P_i C(x_i, x_j) + Q = C(x_0, x_j),\ j = 1, 2, \ldots n \quad \ldots(4)$$

$$\sum_{i=1}^{n} P_i = 1, \quad \ldots(5)$$

where $C(x_i, x_j)$ is the co-variance function of $Z(x_i)$ and $Z(x_j)$ in Equation (4). Equations (4) and (5) are combined to get the weighting coefficient $P_i(i = 1, 2, \ldots, n)$ and Lagrange coefficient *Q*. Then, the interpolation estimation of any point within the research area can be obtained by Equation (3).

The Kriging interpolation method is employed to reflect the accumulation of $PM_{2.5}$ and the changes in its concentration in different areas. The landscape's influence on $PM_{2.5}$ transport is also determined. Therefore, the air pollution emission is influenced by both the transport of air pollution from external sources, and the diffusion of air pollution from internal sources.

# RESULTS AND DISCUSSION

## Pollution Characteristics

Data was collected from Yaoshan Station, Longyin Station, Guilin Environmental Monitoring Station, and No. 8 Middle School Station from 2014 to 2019, and then the data was analyzed to determine changes in $PM_{2.5}$ in different regions. As shown in Fig. 2, the Yaoshan Station presented lower concentrations. The $PM_{2.5}$ concentrations at this station were highest from December to January of the following year and lowest from June to July.

The pollution and meteorological conditions differed significantly from March to August (Period 1) and September to February of the following year (Period 2). Table 2 summarizes the results from Fig. 2. The atmospheric pressure is less correlated with the meteorological parameter ($PM_{2.5}$, $PM_{10}$), and the humidity is directly related to rainfall. The corresponding statistical results were not listed in Table 2.

(1) $PM_{2.5}$ concentration: During Period 1, $PM_{2.5}$ concentrations were greater than 70 $\mu g.m^{-3}$ and less than 20

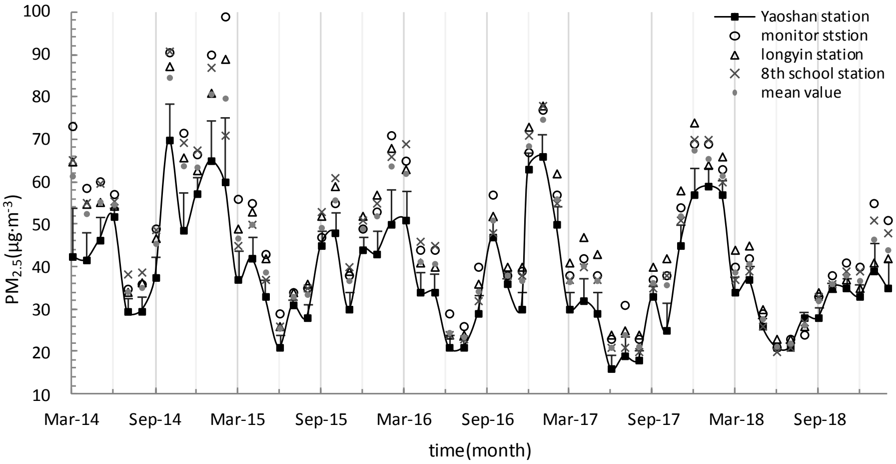


Fig. 2: Comparison of atmospheric environmental quality data of fixed stations in 2014-2019.

$\mu g.m^{-3}$, and between these two values accounted for 2%, 44%, and 54% of the observed $PM_{2.5}$ concentrations, respectively. During Period 2, $PM_{2.5}$ concentrations were greater than 70 $\mu g.m^{-3}$ and less than 20 $\mu g/m^3$, and between these two values accounted for 21%, 20%, and 59%, of the observed $PM_{2.5}$ concentrations, respectively.

(2) Wind direction: During Period 1, eight wind directions had relatively uniform values, with westerly winds and northwesterly winds occurring 4% and 5% of the time, respectively. During Period 2, northerly and northwesterly winds were most frequent and accounted for 43% and 25% of all the winds, respectively.

(3) Wind speed: During Period 1, weak winds occurred the most frequently. As shown in Table 2, 95% of the observed wind was less than 3.5 $m.s^{-1}$. During Period 2, strong winds occurred with greater frequency, and only 83% of the observed winds were less than 3.5 $m.s^{-1}$.

(4) Temperature: During Period 1, the temperatures between 15°C and 30°C accounted for 72% of the observed temperature. Temperatures below 15°C and above 30°C accounted for 16% and 12%, respectively. During Period 2, the temperatures between 10°C and 25°C accounted for 62% of the observed temperature, while temperatures below 10°C and above 25°C accounted for 25% and 13%, respectively.

(5) Rainfall: During Period 1, there was no rainfall 41% of the time. Rainfall between 0.1 and 20 mm occurred on 56% of the days, and more than 20 mm of rainfall occurred on 3% of the days. During Period 2, there was no rainfall 79% of the time, rainfall between 0.1 and 20 mm occurred 21% of the time, and more than 20 mm rainfall occurred 0% of the time.

To summarize, Period 1 typically had temperatures ranging from 15°C to 30°C. This period also had weak, uniform wind directions, larger amounts of precipitation, bad meteorological conditions for pollutant diffusion, and low $PM_{2.5}$ concentrations. Period 2 primarily had temperatures between 10°C and 25°C, strong northeasterly and northerly winds, little rainfall, good meteorological conditions for pollutant diffusion, and high $PM_{2.5}$ concentrations.

Table 2: Proportion of pollution characteristics in Guilin from July 2014 to June 2019.

| $PM_{2.5}$ ($\mu g/m^3$) | Period one (%) | Period two (%) | wind direction | Period one (%) | Period two (%) | wind speed (m/s) | Period one (%) | Period two (%) | temperture (℃) | Period one (%) | Period two (%) | rainfall (mm) | Period one (%) | Period two (%) |
|---|---|---|---|---|---|---|---|---|---|---|---|---|---|---|
| 0~20 | 44% | 20% | N | 12 | 25 | 0~0.5 | 27 | 12 | 0~5 | 0 | 2 | 0 | 41 | 79 |
| 21~30 | 23% | 15% | NE | 20 | 43 | 0.6~1.0 | 26 | 20 | 6~10 | 3 | 23 | 0.1~1 | 21 | 9 |
| 31~40 | 16% | 16% | E | 9 | 5 | 1.0~1.5 | 13 | 14 | 11~15 | 13 | 24 | 1~2 | 8 | 3 |
| 41~50 | 8% | 1% | SE | 10 | 4 | 1.6~2.0 | 11 | 11 | 16~20 | 12 | 17 | 2~3 | 4 | 3 |
| 51~60 | 5% | 15% | S | 17 | 3 | 2.1~2.5 | 8 | 12 | 21~25 | 29 | 21 | 3~5 | 6 | 2 |
| 61~70 | 2% | 12% | SW | 23 | 6 | 2.6~3.0 | 6 | 9 | 26~30 | 31 | 10 | 5~10 | 7 | 3 |
| 71~90 | 2% | 11% | W | 4 | 5 | 3.1~3.5 | 4 | 8 | 31~35 | 11 | 3 | 10~20 | 10 | 1 |
| ≥90 | 0% | 10% | NW | 5 | 9 | ≥3.6 | 5 | 14 | ≥35 | 1 | 0 | >20 | 3 | 0 |

Note: Period 1 is from March to August, and Period 2 is from September to February of the following year.

The research area is located in a subtropical zone, with little demand for heat in the winter and little seasonal difference in atmospheric pollution emissions. Period 1 had more unfavorable meteorological conditions for pollutant diffusion than Period 2, but the air quality was better. This indicates that the transport of pollutants from external sources needs to be focused on.

Table 3 showed the variation of $PM_{2.5}$ concentration from December 8 to 19 in 2019. As a background station, the variation of $PM_{2.5}$ concentration at Yaoshan station was quite different from the other three stations. In the monitoring period, $PM_{2.5}$ concentration at Yaoshan station increased rapidly compared to other stations. After that, $PM_{2.5}$ concentration at the other three stations just began to increase, which reflected the spatial differences of stations.

**Analysis of External Source Transmission**

The HYSPLIT4 model was used to calculate the backward air mass trajectory in the research area, while the PSCF and CWT methods were used to locate and quantify the trajectory sources.

**Analysis of trajectory simulation results:** The first simulation used the Guilin Environmental Monitoring Station as the target. The simulated altitude was 1000 m, which corresponds to 700 m in Guilin. The simulation ran from July 1, 2017, to June 30, 2018, and 48 hours was used as the backward trajectory parameter. The TSV changed over 30%, indicating an acceptable allocated clustering number. The 365-day air mass trajectory lines were organized into three categories: Trajectories ①, ② and ③ (Fig. 3).

Trajectory fractal number and spatial distribution are shown in Table 4.

The majority of the air masses were transported along Trajectory ②. This trajectory also had the highest $PM_{2.5}$ concentrations. The two parameters during Period 2 were higher than those in Period 1, which demonstrates better atmospheric quality during Period 1 (Table 2).

Trajectory ① originated from the south of the research area, and 25.62% of the air masses were transported along this path. The average concentration of $PM_{2.5}$ for this trajectory was 39.47 $\mu g.m^{-3}$, the lowest among the three trajectories. Its daily frequency of pollution was 12.63%. The trajectory ②was the largest and originated from the northeast. Its average concentration of $PM_{2.5}$ was 45.94 $\mu g.m^{-3}$, however, the daily frequency of pollution was 14.41%, which was significantly higher than trajectories ① and ③. The trajectory ③ had a length of 662.9 km and originated from the southwest, and had the least quantity of air masses (11.29%). Its average concentration of $PM_{2.5}$ was 55.27 $\mu g.m^{-3}$, however, its daily frequency of pollution was only 9.7%.

Yaoshan station was regarded as the background value station of external pollution. The clustering results of the air masses and $PM_{2.5}$ concentrations were used to divide pollution sources into internal and external sources and calculate their proportion. The results are shown in Table 5.

External sources were responsible for more than 76% of the pollution, on average. Referring back to Table 4, the air quality was good, and the pollution in period 1 was generally lower.

Table 3: $PM_{2.5}$ concentration at four stations from December 8 to 19 in 2019.

| $PM_{2.5}$($\mu g.m^{-3}$) | 8th School station | Longyin station | Monitor station | Yaoshan station |
|---|---|---|---|---|
| Dec-8 | 31 | 34 | 32 | 66 |
| Dec-9 | 38 | 41 | 39 | 72 |
| Dec-10 | 75 | 75 | 68 | 90 |
| Dec-11 | 92 | 93 | 89 | 123 |
| Dec-12 | 94 | 101 | 98 | 128 |
| Dec-13 | 98 | 103 | 93 | 93 |
| Dec-14 | 129 | 136 | 121 | 85 |
| Dec-15 | 128 | 134 | 122 | 68 |
| Dec-16 | 95 | 98 | 96 | 45 |
| Dec-17 | 82 | 88 | 85 | 36 |
| Dec-18 | 75 | 78 | 76 | 30 |
| Dec-19 | 49 | 65 | 59 | 42 |

In the second period, pollution was more severe. External sources contributed 84.7% of the total pollution, and Trajectory ① accounted for the highest proportion (95.1%). External sources accounted for 83% of the annual pollution, of which Trajectory ③ accounted for the highest proportion (94.2%). The contribution of external pollution from the “Xiang Gui corridor” (Trajectory②) was 83.2%. Trajectory ② mainly represented pollution from external sources. In Trajectory ③, the contribution of pollution from external sources was high, but few air masses were transported along this trajectory. Therefore, this trajectory could not represent the primary cause of pollution in the study region.

The majority of the air masses traveled along Trajectory ②. It is not surprising that this trajectory carried more pollutants and had higher $PM_{2.5}$ concentrations. Trajectory ③also had high concentrations of $PM_{2.5}$, but fewer air masses were transported along this trajectory. The trajectory 1 concentration of $PM_{2.5}$ was close to the value of the target area.

Trajectories ① and ③ had longer transmission distances and low $PM_{2.5}$ concentrations. These trajectories do not transport enough pollution from external sources and should be taken as the main direction for the diffusion of internal source pollution in the research area. Additionally, by comparison in Table 4, Fig. 3, and Fig. 1, it was found that Trajectory ② was coincident with the “Xiang-Gui Corridor.” It showed that this area should be taken as the key point for impact analysis of topographical changes.

**PSCF result analysis:** The daily mean concentration of $PM_{2.5}$ (75 $\mu g.m^{-3}$) was used as the threshold. The total residence time of the trajectory in the grid and the daily average value was 48 h. The simulation was run for 365 days, and 10 days was used as the average residence time in the grid. To

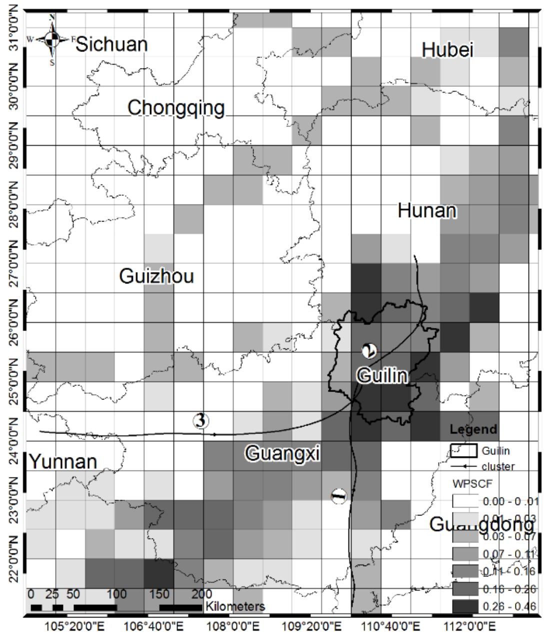


Fig. 3: The WPSCF distribution and clustering analysis results of backward trajectory

Table 4: Result analysis of trajectory clustering.

| cluster | period one trajectory (number) | period one $PM_{2.5}$ ($\mu g/m^3$) | period two trajectory (number) | period two $PM_{2.5}$ ($\mu g/m^3$) | year trajectory (number) | path length（km） | year trajectory number ratio （%） | year $PM_{2.5}$ ($\mu g/m^3$) | PM2.5>75 （number） | day pollution frequency （%） |
|---|---|---|---|---|---|---|---|---|---|---|
| 1 | 34 | 47.9 | 61 | 33.21 | 95 | 448.5 | 25.62 | 39.47 | 12 | 12.63 |
| 2 | 125 | 54.64 | 104 | 35.48 | 229 | 276.2 | 63.09 | 45.94 | 33 | 14.41 |
| 3 | 23 | 75.33 | 18 | 29.63 | 41 | 662.9 | 11.29 | 55.27 | 4 | 9.7 |
| all | 182 | 57.37 | 183 | 34.15 | 365 | 1387.6 | 100 | 45.05 | 50 | 13.71 |

Note: Period 1 is from March to August, and Period 2 is from September to February of the following year

Table 5: Proportion of internal and external pollution sources in different periods.

| cluster | Period 1 $PM_{2.5}$ proportion of external pollution sources | Period 1 $PM_{2.5}$ proportion of internal pollution sources | Period 2 $PM_{2.5}$ proportion of external pollution sources | Period 2 $PM_{2.5}$ proportion of internal pollution sources | Annual $PM_{2.5}$ proportion of external pollution sources | Annual $PM_{2.5}$ proportion of internal pollution sources |
|---|---|---|---|---|---|---|
| 1 | 76% | 23% | 95.10% | 4.90% | 73.80% | 26.20% |
| 2 | 76.40% | 23.60% | 84% | 16% | 83.20% | 16.80% |
| 3 | 80.10% | 19.90% | 88% | 12% | 94.20% | 5.80% |
| ALL | 76.70% | 23.30% | 84.70% | 15.30% | 83% | 17% |

avoid distortion caused by too high PSCF values in grids $n_i$, empirical weight function, $W_i$, was introduced:

$$W_i = \begin{cases} 1.0 & n_i > 10 \\ 0.7 & 5 < n_i \leqslant 10 \\ 0.42 & 2 < n_i \leqslant 5 \\ 0.17 & n_i \leqslant 2 \end{cases} \quad . \qquad \ldots (6)$$

This formula indicates values of $W_i$ when $n_i$ trajectories pass through grids $i$ at the above time points. The PSCF value is then given by $WPSCF_i = PSCF_i \times W_i$.

The WPSCF values were distributed as the grid values of Fig. 3. The northeast grid had large gray values, which indicated that the air pollution was transported along Trajectory ②. Therefore, the source was located in the grid in the northeast of Trajectory ②. Trajectories ① and ③ had smaller grid values outside the research area and larger values within the research area, which suggests that the internal pollution source was consistent with the results obtained from the trajectory data.

**CWT results analysis:** The PSCF method was used to analyze the influence of pollution in the research area from a semi-quantitative perspective. The CWT method was also used to determine the source of the pollutants. The backward trajectories are shown in Fig. 4. The trajectories from the northeast and south are presented as dark grids in a consistent direction of the cluster trajectory line. By comparison, areas with dark grids could coincide in Fig. 3 and Fig. 4, indicating that the sources were located in the northeast and south of the research area.

**Characteristics of external source transmission:** According to the WCWT distribution and clustering results of backward trajectories, it is known that (1) Trajectory ② accounted for 63.09%, with an average $PM_{2.5}$ concentration of 45.94 $\mu g.m^{-3}$. (2) The dark grids were in the northeast, implying that the "Xiang-Gui Corridor" is the source of the pollutants. (3) Dark grids were also located in the north and northeast of the research area, where there is a lot of industries. In other areas of the research region, the darker grids coincided with trajectories ① and ③.

Based on the above analysis, it can be inferred that the air pollution in the research area was emitted from a combination of external sources (i.e., from the "Xiang-Gui Corridor") and internal sources.

## Analysis of Internal Source Pollution

The previous section analyzed external sources of air pollution and air mass trajectories. It is natural to next consider how external and internal sources jointly impact pollution using a spatial interpolation method.

As shown in Table 4, $PM_{2.5}$ concentrations peaked between September 2017 and February 2018. Four pollution events were selected to interpolate the mean $PM_{2.5}$ concentrations from 19 stations using the Kriging interpolation method. The four events chosen were from October 31 to November 9, December 13 to December 22, December 28 to January 6, and January 23 to February 1. The results are shown in Fig. 5.

$PM_{2.5}$ concentrations were high in Quanzhou County and urban areas. However, the $PM_{2.5}$ concentration in Longsheng County and Gongcheng County was relatively low. This is consistent with Fig. 3 and Fig. 4, which showed that the external source of pollution came from the northeast. During the four pollution events, Ziyuan County, the northeast of Xing'an County, and Guanyang in the "Xiang-Gui Corridor" showed relatively low $PM_{2.5}$ concentrations.

The distribution of the blue belt varied with the pollution events. Its core area was northeast of Xing'an County, with the Yuechengling Mountains to the northwest and the Ocean Mountains in the Dupangling Mountains to the southeast. The peaks affect the direct transport of the air masses and form obvious weakening zones. The Yaoshan Mountains to the northeast of the urban areas act as barriers and prevent

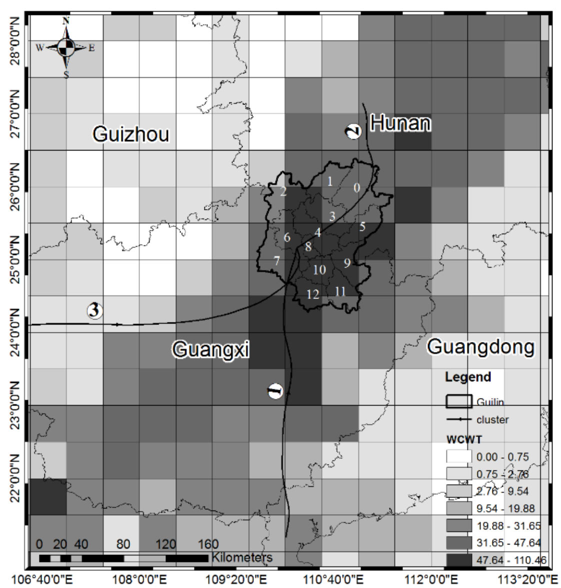


Note: 0 Quanzhou County, 1 Ziyuan County, 2 Longsheng County, 3 Xing'an County, 4 Lingchuan County, 5 Guanyang County, 6 Lingui County, 7 Yongfu County, 8 the urban area, 9 Gongcheng County, 10 Yangshuo County, 11 Pingle County, and 12 Lipu County

Fig. 4: The WCWT distribution and clustering analysis results of backward trajectory

the air masses from directly entering the urban areas, causing the four pollution events.

The four periods in Fig. 5 all showed that Quanzhou County in the northeast and the urban areas in the center contain high concentrations of pollution. This shows the effect of the internal and external sources and suggests that while Quanzhou County is affected by the northeastern air mass, the internal sources also contribute toward the accumulation of pollution in the urban areas.

## CONCLUSIONS

This study focused on the sources and transport of $PM_{2.5}$ in the city of Guilin. A combination of $PM_{2.5}$ daily average and meteorological parameters data, and simulations using the HYSPLIT model were used to analyze pollutant sources, internal source diffusion, and the effect of topography on pollutants in the research area. Conclusions could be drawn as follows.

1. From 2014 to 2019, heavy pollution periods in the research area occurred from September to February.

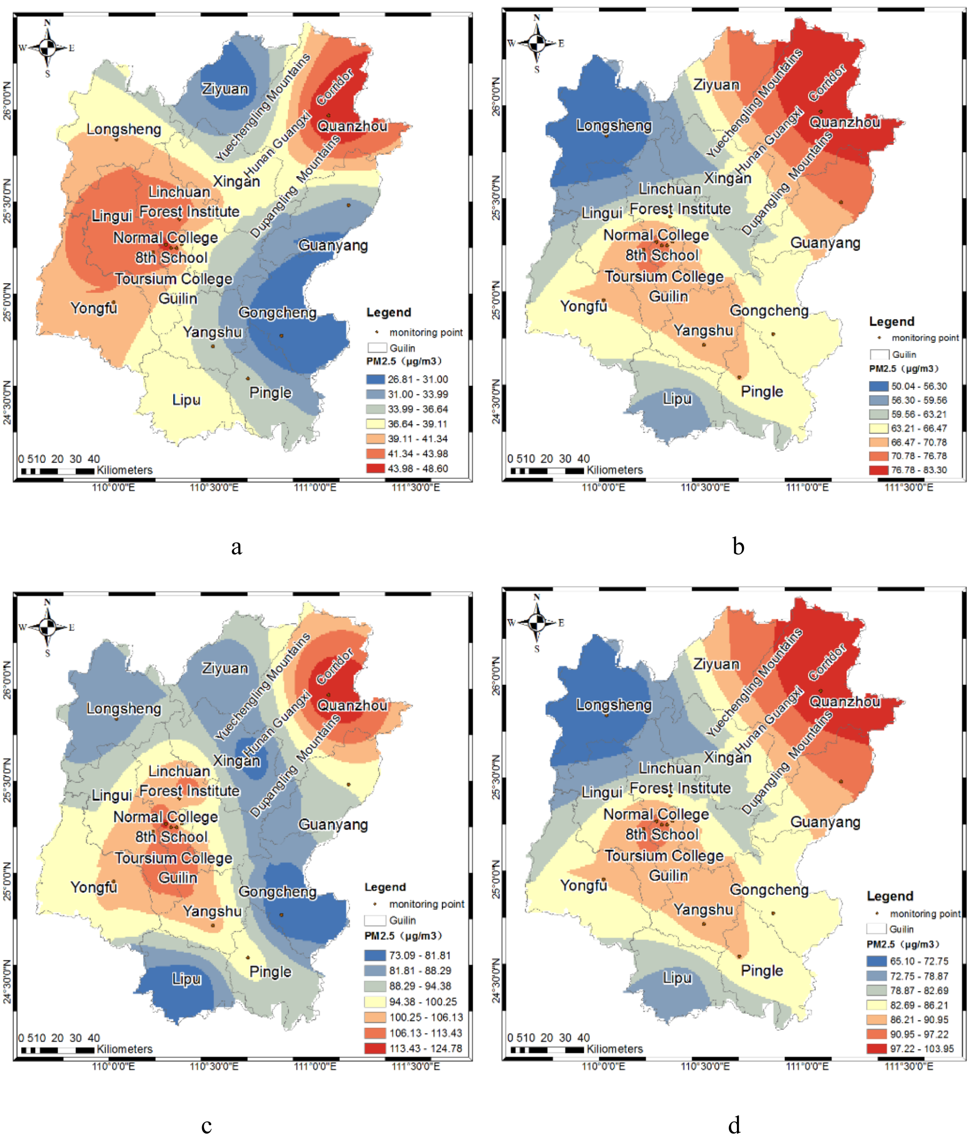


Note: A: October 31 to November 9, B: December 13 to December 22, C: December 28 to January 6, D: January 23 to February 1

Fig. 5: The interpolation results of four pollution processes in Winter in Guilin.

2. External sources were predominantly from the northeast direction, and the trajectory of the pollutants coincided with the "Xiang-Gui Corridor." Potential source areas were concentrated in industrial regions in the Hunan Province, which lies to the northeast of the research area. The internal sources were located to the south and southeast. In particular, pollution originated in Yongfu County, Lipu County, and Pingle County.
3. Multiple pollution events showed that the temporal and spatial characteristics of pollutant transport were affected by special terrain. The "Xiang-Gui Corridor" was affected by external sources in the northeast and formed a regional center of atmospheric pollution. The urban areas, which were under the influence of internal, southern, and southeastern sources, formed a second regional center.

## ACKNOWLEDGMENTS

This work was supported by the National Natural Science Foundation of China [grant number 41967042]; the State-supported Special Fund Project for Local Science and Technology Development [grant number ZY1949005]; the Guangxi Key Research and Development Program [grant number AB18221108]; the Guilin Key Scientific Research and Technological Development Program (grant number 20190213-1).

## REFERENCES

Arif, M., Kumar, R., Kumar, R., Eric, Z. and Gourav, P. 2018. Ambient black carbon, $PM_{2.5,}$ and $PM_{10}$ at Patna: Influence of anthropogenic emissions and brick kilns. Sci. Total Environ., 624: 1387-1400.

Bai, X., Zhang, Y., Wang, C. and Tan, Y. 2016. Analysis of climate resources impact on Guilin international resort tourism development. Int. J. Environ. Protect. Policy, 4(6): 196-200.

Cui, J., Lang, J., Chen, T., Cheng, S. and Chen, S. 2019. Emergency monitoring layout method for sudden air pollution accidents based on a dispersion model, fuzzy evaluation, and post-optimality analysis. Atmos. Environ., 222: 117124.

Jiang, N., Yin, S., Guo Y., Li, J., Kang, P., Zhang, R. and Tang, X. 2018. Characteristics of mass concentration, chemical composition, source apportionment of PM25 and PM10, and health risk assessment in the emerging megacity in China. Atmos. Pollut. Res., 9(2): 309-321.

Liu, B., Wu, J., Zhang, J., Wang, L., Yang, J., Liang, D., Dai, Q., Bi, X., Feng, Y., Zhang, Y. and Zhang, Q. 2017. Characterization and source apportionment of PM2.5 based on error estimation from EPA PMF 5.0 model at a medium city in China. Environ. Pollut., 222: 10-22.

Liu, N., Yu, Y., He, J. and Zhao, S. 2013. Integrated modeling of urban-scale pollutant transport: application in a semi-arid urban valley, Northwestern China. Atmos. Pollut. Res., 4(3): 306-314.

Luan, T., Guo, X., Guo, L. and Zhang, T. 2018. Quantifying the relationship between PM2.5 concentration, visibility, and planetary boundary layer height for long-lasting haze and fog-haze mixed events in Beijing. Atmos. Chem. Phys., 18(1): 203-225.

Mukherjee, A. and Agrawal, M. 2018. Assessment of local and distant sources of urban $PM_{2.5}$ in the middle Indo-Gangetic plain of India using statistical modeling. Atmos. Res., 213: 275-287.

Perrone, M.G, Vratolis, S,. Georgieva, E., Török, S., Šega, K. Veleva, B.. Osán, J., Bešlić, I., Kertész, Z., Pernigotti, D., Eleftheriadis, K. and Belis, C. A. 2018. Sources and geographic origin of particulate matter in urban areas of the Danube macro-region: The cases of Zagreb (Croatia), Budapest (Hungary), and Sofia (Bulgaria). Sci. Tot. Environ., 619-620: 1515-1529.

Sun, K., Liu, X., Gu, J., Li, Y., Qu, Y., An, J. Wang, J. 2015. Chemical characterization of size-resolved aerosols in four seasons and hazy days in the megacity Beijing of China. J. Environ. Sci., 32: 5-167.

Sun, R., Fan, L. and Chen, Z., 2019. Temporal and spatial distribution characteristics of atmospheric PM 2.5 concentrations in Guiyang, China. Nat. Environ. Pollut. Technol., 18(2).

Wang, M., Cao, C., Li, G. and Singh, R. P. 2015. Analysis of a severe prolonged regional haze episode in the Yangtze River Delta, China. Atmos. Environ., 102: 112-121.

Yang, X., Wu, Q., Zhao, R., Cheng, H., He, H., Ma, Q., Wang, L. and Luo, H. 2019. A new method for evaluating winter air quality: PM2.5 assessment using Community Multi-Scale Air Quality Modeling (CMAQ) in Xi'an. Atmos. Environ., 4: 18-28.

Yang, Y., Christakos, G., Yang, X. and He, J. 2018. Spatiotemporal characterization and mapping of PM2.5 concentration in southern Jiangsu province, China. Environ. Pollut., 234: 794-803.

Zdun, A., Rozwadowska, A. and Kratzer, S. 2016. The impact of air mass advection on aerosol optical properties over Gotland (Baltic Sea). Atmos. Res., 182: 142-155.

Zhang, Q., Xue, D., Liu, X., Gong, X. and Gao, H. 2019. Process analysis of PM2.5 pollution events in a coastal city of China using CMAQ. J. Environ. Sci., 5(79): 225-238.

Zhang, Y., Li, X., Nie, T., Qi, J., Chen, J. and Wu, Q. 2018. Source apportionment of PM2.5 pollution in the central six districts of Beijing, China. J. Clean. Prod., 174: 661-669.

Zhao, Y. Z., Man, S. W. and Kwon, H. L. 2015. Estimation of potential source regions of PM2.5 in Beijing using backward trajectories. Atmos. Pollut. Res., 6(5): 173-177.

Zhou, Y., Zhou, J. and Xiao, R. 2016. Research for regional contribution rate of internal source and external source of PM2.5 based on a set pair analysis method. Meteorol. Environ. Res., 2: 36-40+44.